Draft version October 22, 2026
Typeset using LaTeX **default** style in AASTeX7.0.1

arXiv:2610.29006v1 [astro-ph.SR] 21 Oct 2026

Rotation in the Lagoon Nebula with K2

L. M. Rebull,[1] A. M. Cody,[2] L. Venuti,[2,3] S. Thanvantri,[4] and A. Thanvantri[5]

[1] *Infrared Science Archive (IRSA), IPAC, MS 100-22, 1200 E. California Blvd., California Institute of Technology, Pasadena, CA 91125, USA*

[2] *SETI Institute, 339 Bernardo Ave., Suite 200, Mountain View, CA 94043, USA*

[3] *Visiting Fellow, School of Physics, UNSW Science, Kensington, NSW 2052, Australia*

[4] *Department of Computer Science, Princeton University, 35 Olden St, Princeton, NJ 08544, USA*

[5] *Harvard John A. Paulson School of Engineering and Applied Sciences, 150 Western Ave, Allston, MA 02134 USA*

ABSTRACT

A low-mass star's rotation rate drives its magnetic field, and in the case of young stars, also affects accretion and planetary formation. Observations of the rotation rates of young stars help constrain models of star and planet formation. We present rotation rates from K2 observations of stars in the ∼1-2 Myr Lagoon Nebula, one of the youngest clusters with space-based rotation rates available. From 414 light curves we obtain reliable rotation periods for 325 stars; 124 of them are disk-bearing and 201 are disk-free. This constitutes a significant increase in the collection of K2 rotation rates available for ∼1-5 Myr stars. The overall distribution is broadly consistent with expectations, in that the slowest rotators are mid-K and both lower and higher masses are on average faster rotating. There is weak evidence that disked stars rotate more slowly. There are a few complex periodic variables, but they appear to be surprisingly high mass compared to prior known examples of this kind of object.

1. INTRODUCTION

The evolution of stellar rotation rates during the first few million years of a star's life is important for understanding how – and whether – stars form planets. For young low-mass stars, cool magnetospheric starspots rotating into and out of view create changes in the measured light from the star, variations that are large and easy to measure compared to planetary transits. For stars that still have circumstellar disks, the interaction between the star and its disk as the young stellar object (YSO) contracts onto the main sequence is revealed via brightness fluctuations arising from photospheric cool spots or accretion hot spots rotating into and out of view. Non-uniformities in the disk or accretion columns can occult the central YSO from our perspective, and changes in the accretion rate can all result in changes in the light we detect. If we can determine the stellar rotation rate despite these flickering contributions, conservation of angular momentum through these early phases of a star's life can be revealed in the evolution of the stellar rotation rate through disk dispersal and possibly planet formation. The variations of YSOs are easily detected by missions designed for planet hunting, like NASA's K2 (S. B. Howell et al. 2014).

Studying stellar rotation rates in the youngest clusters is complicated not only because of the often stochastic contribution from disks and accretion, but because of the dusty natal environments. Reddening affects the measured colors and brightnesses, which affects the inferred distances, temperatures, masses, and ages. Rotation periods are often the quantity known with the highest accuracy and precision in young stars.

The Lagoon Nebula is a high-mass star-forming region located in projection near the Galactic Center. NGC 6530 is an open cluster slightly in front of the nebulosity that is also part of M8. Stars in M8 are known to be young (∼1-2 Myr; L. Prisinzano et al. 2019), but it is relatively far away at ∼1250 pc (L. Prisinzano et al. 2019). In L. Venuti et al. (2021, 2024), we have discussed results from multicolor ground- and space-based monitoring of the Lagoon Nebula, and explored the influence of environment and mass on circumstellar disk accretion. In L. M. Rebull et al. (2026), we presented a catalog of literature-selected YSOs optimized for this region and assembled SEDs from archival photometric data. The work in the current paper depends on the catalog from L. M. Rebull et al. (2026), relying on the analysis there for SEDs, disk identification, and reddening estimates. Figure 1 shows the location on the sky of the YSOs from this catalog.

In this paper, we use the K2 observations of the Lagoon Nebula originally presented in L. Venuti et al. (2021) to infer rotation rates for the YSOs. There are 414 unique light curves (these objects are highlighted in Fig. 1), and

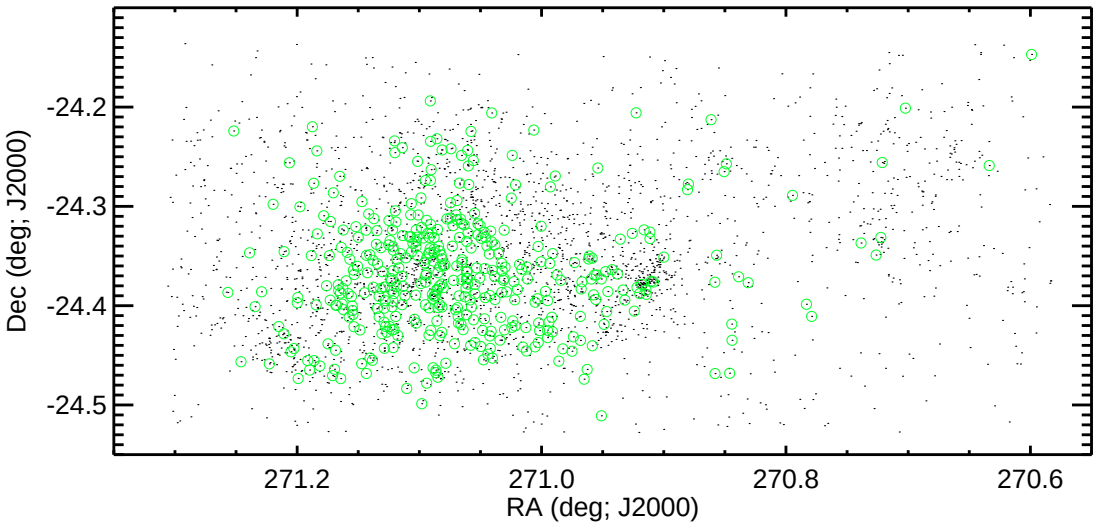

Figure 1. A plot on the sky of the YSO candidates in the master catalog from L. M. Rebull et al. (2026) (black dots) with the targets from this paper (those with K2 light curves) indicated via an additional green circle.

the Lagoon is one of the youngest clusters for which there are substantial numbers of space-based rotation rates now available. The confusion arising from the surface density of sources and the stochastic contributions to the light curves from accretion and circumstellar disks both make this analysis difficult.

We begin in Sec. 2 by summarizing the ancillary data obtained from L. M. Rebull et al. (2026) and the data directly relevant to the analysis in this paper; we also summarize the K2 data reduction and our period-finding approach in this section. Sec. 3 discusses the distribution of P vs. $(V-K_s)_0$ for the Lagoon on its own and in context with other clusters. We also discuss the influence of disks. Sec.4 highlights a few of the other kinds of light curves, including particularly the complex periodic variables identified here. Then we summarize the results in Sec 5.

2. OBSERVATIONS AND DATA REDUCTION

2.1. *Ancillary Data*

We assembled a large catalog of literature YSOs in L. M. Rebull et al. (2026), optimized for the region encompassed by the K2 data. There, we also identified the YSOs with disks, and resolved source confusion issues within that catalog as best we could. The K2 pixels are large enough ($\sim 4''$), and the source surface density is high enough, that we used our master catalog (along with selected image inspection) to identify light curves likely to be subject to spatial confusion issues.

Since we ultimately needed V magnitudes to put these stars in the same rotation parameter space as similar data from other clusters, we specifically sought measured V from the literature. More than 90% of the stars with light curves have a measured V magnitude. As can be seen in L. M. Rebull et al. (2026), the SEDs are in general very well defined in the optical. For the stars without measured V in L. M. Rebull et al. (2026), as in other of our papers (*e.g.*, L. M. Rebull et al. 2022), we interpolated a value for V from a fit to the SED. JHK_s measurements come from the Two Micron All-Sky Survey (2MASS; M. F. Skrutskie et al. 2006; 2MASS Team 2020).

As discussed in L. M. Rebull et al. (2026), the reddening in this region is inhomogenous and can be substantial. If we have a spectral type estimate, we can compare the observed $(V-K_s)$, or the interpolated $V-$ the observed K_s, to the expected $(V-K_s)$ for the spectral type to get an estimate of the reddening.

We have spectral type estimates for $\sim$90% of the sample with light curves. For the remaining stars, if we have JHK_s for the stars (which we do for most of the remaining catalog), we can place the stars on a $J-H$ vs. $H-K_s$ diagram, then shift them back along the reddening law derived by R. Indebetouw et al. (2008) to the expected JHK_s colors for young stars from M. J. Pecaut & E. E. Mamajek (2013) or the T Tauri locus from M. R. Meyer et al. (1997), and convert to $E(V-K_s)$ via $A_K = 0.114A_V$ (J. A. Cardelli et al. 1989).

As discussed in L. M. Rebull et al. (2026), the reddening as calculated via those two methods may be very different. Figures 2 and 3 are similar to those in L. M. Rebull et al. (2026) but only include the subsample with light curves. The $E(V-K_s)$ as calculated from JHK_s is somewhat correlated with the $E(V-K_s)$ from spectral type, but the correlation is not particularly strong. The $E(V-K_s)$ as calculated from JHK_s seems to peak more or less near 0; however, as described in L. M. Rebull et al. (2026), the set of values at exactly 0 are affected by cases where the routine failed to converge on $A_V>0$, or failed to converge at all. In contrast, when $E(V-K_s)$ is calculated using spectral types, the distribution peaks at ∼1.25-1.3 mag, comparable to that for the entire catalog. There is a long tail to large extinction values, though not as long or large as the entire catalog in L. M. Rebull et al. (2026) – this is expected, given that the criteria to be included here include a viable K2 (optical) light curve, so very embedded objects are excluded.

In the end, the only stars with nominal light curves for which we lack estimates of reddening are three for which we are missing K_s measurements due to source confusion. Since 2MASS can't resolve these stars, certainly K2 can't either, and the K2 light curves are also negatively impacted by source confusion. These stars' light curves were functionally identical to that from their apparent companion and were dropped.

Table 1 includes the best available K_s, the observed V (when available), the best available $(V-K_s)$ and $(V-K_s)_0$, and the indication of whether or not the star has a disk from L. M. Rebull et al. (2026).

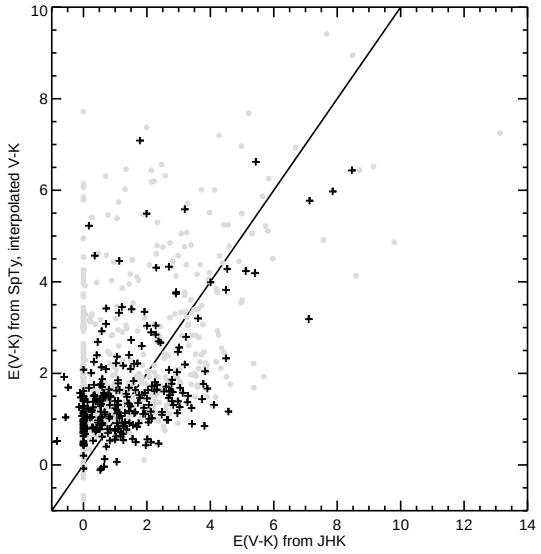

Figure 2. Comparison of $E(V-K_s)$ for stars where the reddening is estimated from the placement in the JHK_s diagram (x-axis) and the $E(V-K_s)$ calculated from the observed K_s, interpolated V, and colors assumed from the spectral type. A 1:1 line is overplotted; the grey underplotted dots are the values from the entire catalog (L. M. Rebull et al. 2026). There is a weak correlation, but it displays less scatter than for the entire catalog from L. M. Rebull et al. (2026).

2.2. *K2 Time Series*

The K2 observations and their data reduction are described in more detail in L. Venuti et al. (2021). In summary, K2 observed the Lagoon nebula region from 2016 April 21 – July 1. There were some individual stars targeted with postage stamps, but most of the cluster was monitored via a superstamp. The K2 campaign sampled every ∼30 minutes for ∼70 days.

Aperture photometry was extracted for the targets, with the best possible aperture selected individually for each target. The light curves we generated are available as part of the K2YSO high-level science product in the Mikulski Archive for Space Telescopes: 10.17909/44f5-5e13 (A. M. Cody et al. 2023; A. M. Cody & L. A. Hillenbrand 2018; L. Venuti et al. 2021; A. M. Cody et al. 2022).

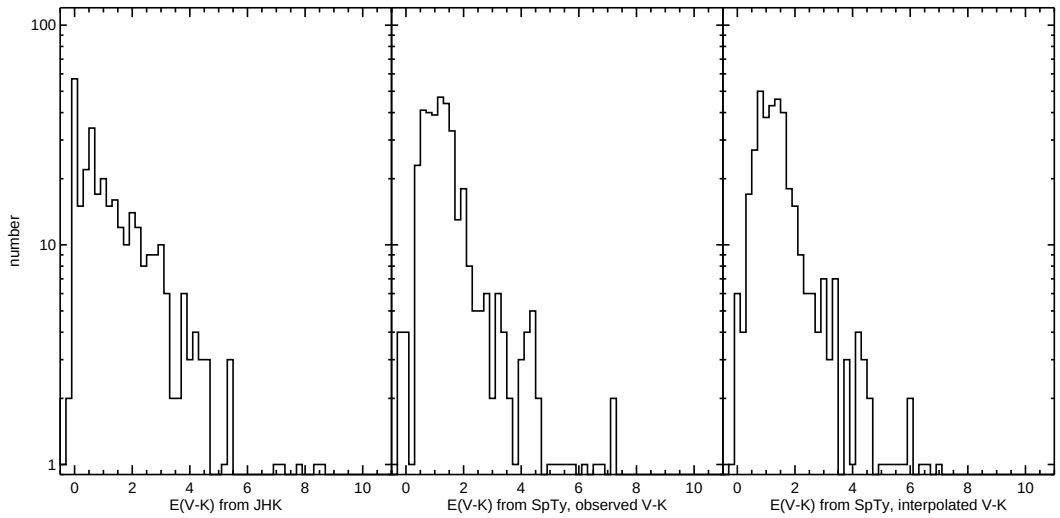

Figure 3. Comparison of $E(V-K_s)$ for stars where the reddening is estimated from the placement in the JHK_s diagram (left), the $E(V-K_s)$ calculated from the observed V and K_s (middle) and colors assumed from the spectral type, and the $E(V-K_s)$ calculated from the interpolated V and colors assumed from the spectral type (right). See the text for more discussion.

2.3. *ZTF Time Series*

Because the source surface density is so high and the K2 pixels are so large, in some cases, source confusion posed an issue. The data from the Zwicky Transient Facility (ZTF; E. C. Bellm et al. 2019; F. J. Masci et al. 2019; ZTF Team 2026) are high enough spatial resolution that in many cases, it can resolve the sources, but it does not have as high sensitivity or as rapid time sampling in comparison to K2. ZTF typically samples once per night or few nights, over 8 years, in g and/or r-band, and the pipeline photometry typically has scatter of at least a few percent. Because the sampling is nightly, there is substantial aliasing with 1 d, 0.5 d, etc. ZTF extracted light curves are housed at IRSA (ZTF Team 2026); we searched by position to find the closest object to our target.

We searched for periods in these data using the same approach as we used for the K2 data (see next subsection), but because of the wildly different sampling and sensitivity, we only used ZTF to confirm periods from K2, or to allocate the period(s) from K2 appropriately to stars resolved in ZTF but unresolved by K2. These cases are noted in Table 1 where relevant. In about one-third of the stars with available ZTF light curves, corroborating evidence for the K2 period can be found in one or both of the available ZTF light curves.

Public ZTF data are not available for every target. In one case, where there was no public ZTF data but it still seemed that ground based data would be particularly helpful, we consulted ASAS-SN (B. J. Shappee et al. 2014; C. S. Kochanek et al. 2017) to check on the K2 period. This is noted in Table 1.

2.4. *Measurement of Rotation Periods*

To identify significant periods, we used the Lomb-Scargle (J. D. Scargle 1982) approach as implemented by the NASA Exoplanet Archive Periodogram Service[6] (R. L. Akeson et al. 2013). We used the Infrared Science Archive (IRSA) Time Series Tool[7], which employs the same underlying code as the Exoplanet Archive service, but allows for interactive period selection. We generally searched a period range from 0.05 days (1.2 hours) through 20 days. In some cases, we deliberately sought shorter periods where warranted.

For each significant peak, we phased the light curve and examined it, omitting outliers if need be to assess the light curve. Through this process, we identified and omitted factor-of-two aliases and harmonics; we identified and retained additional real periods. We retained up to 4 periods for each star; ∼25% of the periodic light curves have at least two periods, but only ∼3% of the sample have at least four periods.

[6] https://exoplanetarchive.ipac.caltech.edu/cgi-bin/Pgram/nph-pgram
[7] http://irsa.ipac.caltech.edu/irsaviewer/timeseries

Table 1. Contents of Table: K2 Rotation Periods in The Lagoon Nebula

Column	Contents
catnum	IAU-compliant position-based catalog number – also appears in L. M. Rebull et al. (2026)
ra	right ascension (J2000)
dec	declination (J2000)
diskcode	disk code from L. M. Rebull et al. (2026); ≥3 suggests disk based on available information
bestk	best available K_s, in Vega magnitudes
obsv	observed V, when available, in Vega magnitudes
bestvk	best available observed $(V - K_s)$, in Vega magnitudes
bestderedvk	best available dereddened $(V - K_s)_0$, in Vega magnitudes
p1	period in days, taken to be the rotation period of the star when available
p2	second period, in days
p3	third period, in days
p4	fourth period, in days
ztfconf	does information from ZTF confirm this period as derived from K2? only populated if yes
hendp	literature period in days from C. B. Henderson & K. G. Stassun (2012) (when available)
ordenp	literature period in days from C. Ordenes-Huanca et al. (2022) (when available)
dd	if set, light curve is "double dip" type (two dips per cycle)
ddmoving	if set, light curve is "moving double dip" type (two dips per cycle that move with respect to each other)
shch	if set, light curve is "shape changer" type (shape changes over campaign)
batwing	if set, light curve is "batwing" type
beater	if set, light curve is "beater" type (beating apparent in light curve)
complexpeak	if set, light curve is "complex peak" type (structure seen in periodogram peak[s])
resolvedclose	if set, light curve is "resolved close" type (peaks close in periodogram)
resolveddistant	if set, light curve is "resolved distant" type (peaks distant in periodogram)
pulsator	if set, light curve is "pulsator" type (many short-P peaks)
disky	if set, light curve variability resembles those from stars with disks
dipper	if set, light curve is "dipper" type
burster	if set, light curve is "burster" type
binary	if set, light curve is "binary" type – e.g., suggests binarity
iffy	if set, period is "iffy" (uncertain, or may not be rotation)
notes	notes on object's color, light curve, and/or period

We classified the light curves according to the schemes we have established in earlier papers (*e.g.*, L. M. Rebull et al. 2022, and references therein). These classifications are discussed in more detail below and overlap with those from L. Venuti et al. (2021). In most cases, the classifications between the two papers are consistent with each other. In several cases, we had to reassess the classification with respect to the one presented in L. Venuti et al. (2021) – for example, some of the stars that are listed there as not periodic, upon closer consideration here, are periodic.

The periods we derive appear in Table 1, along with the light curve classifications.

2.5. *Comparison to the Literature*

Figure 4 compares the periods obtained here to those found in the literature. In general, there is good agreement.

C. B. Henderson & K. G. Stassun (2012) monitored the region in I_C with observing runs scattered over 6 observing seasons. We merged their catalog with ours in L. M. Rebull et al. (2026). They have 100 targets in common with us and those targets are shown on the sky in Fig. 5; their field of view was smaller than our field. Out of those stars in common, 87 match within 10%, and an additional 6 match within ∼50%. For several of the targets that are mismatched, the periods we find are a factor of two off from that in the literature. For four targets, we report a second period for that star, and in three of the four cases, this second period is closer to the 1:1 line than the first period. In

three cases, we have noted the periods we report as perhaps uncertain, but one of those matches the literature value very well.

C. Ordenes-Huanca et al. (2022) analyzed K_s light curves from the VISTA Variables in the Vía Láctea extension (VVVX; R. K. Saito et al. 2012; D. Minniti et al. 2017). Cross-matching their catalog with ours (see L. M. Rebull et al. 2026) yields 99 targets in common (see Fig. 5). For 50 targets, the periods agree within 10%, with an additional 8 matching within 60%. C. Ordenes-Huanca et al. (2022) report periods for five targets to be >100 d, which cannot be recovered given the ∼70 day K2 baseline. For the remaining 44 discrepant sources, 27 (∼60%) have K2 light curves characteristic of circumstellar disks, where accretion or extinction variability can be seen on top of underlying rotation. This intrinsic disk-related activity, combined with standard ground-based observational constraints (day/night gaps, windowing functions with short campaigns stretching over seasons, and weather/seeing), particularly complicates period retrieval for active young stars. Additionally, six of the mismatches (and one of the matches) have such strong stochastic contributions even in the K2 light curves that we flagged their periods as uncertain. In a few cases where we report a second period, the second period is closer to the 1:1 line than the first period. We note also that several of the particularly poor mismatches have literature periods that cluster near ∼0.8-1 d, suggesting possible daily aliasing in the ground-based data. (This clump includes four of the six targets flagged with uncertain K2 periods.)

Other contributing factors could be the light curves as observed themselves. The VVVX light curves are on the order of 100 epochs spread over 12 years (median time step ∼5 d), to be compared with our ∼3270 epochs over ∼70 days (typical time step ∼30 min); the stars are likely to change more over years than over days, and sparse light curves make it harder to find periods than dense light curves. Moreover, there could be physical changes in the dominant variability source between epochs; C. Ordenes-Huanca et al. (2022) monitored in the NIR and K2 worked in the optical, so if there are small changes in the disk between observation epochs, it could lead to changes in light curve amplitude between optical and K_s. Perhaps related to this concept, interestingly, for two stars (J180405.76-241455.0 and J180413.77-242405.1), we retrieve two different periods. One of those periods is retrieved (in the optical) by C. B. Henderson & K. G. Stassun (2012) and the other (in the NIR) by C. Ordenes-Huanca et al. (2022). (See Table 1 for specifics.)

We conclude that our periods are at least as accurate as those previously reported in the literature.

3. PERIOD DISTRIBUTIONS

3.1. *A First Look*

Figure 6 presents the first look at the distribution of rotation rates as a function of color (a proxy for mass) in the Lagoon Nebula. In this figure, the distribution of rotation rates found in Upper Scorpius (USco; L. M. Rebull et al. 2018) is provided for reference, though a more complete comparison to other clusters will be provided below. USco, at ∼8 Myr, is slightly older than the ∼1-3 Myr Lagoon. USco is significantly closer, so the population for which we have periods is richer and reaches fainter masses. The distributions are roughly comparable – the slowest rotators in the ensemble are near mid-K, $(V-K_s)_0$∼2.5 to 3; the periodic A and F stars are rotating faster than the mid-Ks; the mid-M stars are also rotating faster than the mid Ks.

Figure 6 requires some caveats. Due to the reddening issues discussed above, the $(V-K_s)_0$ colors appear quantized, particularly near $(V-K_s)_0$∼3.5, because the stars are corrected to the expected color based on spectral type, and spectral types are quantized. Figure 6 has stars flagged where the periods may not be as reliable as others here due to noisy data, whether that be inherent noise in the light curve or 'noise' from accretion events; these are also called out in Table 1. These stars are often but not always outliers. These dubious periods are omitted from later plots.

Figure 6 also identifies stars for which periods may be due to pulsation. These pulsators are identified simply by the fact that the periods are very fast (typically fractions of hours to a few hours) and usually there are many viable peaks in the periodogram (often >4 though we only record up to 4). For the 12 possible pulsators identified here, we report 4 periods for 9 of them, but only 3 periods for 1, and only 2 periods for 2; the periods are fast enough that we retained their tentative classification as pulsators. Experience with other clusters (L. M. Rebull et al. 2018, and references therein) suggests that, for these stars so-identified as pulsators, the strongest peak in the power spectrum may be related to the rotation period, in that for most of the stars flagged as possible pulsators, the period corresponding to strongest peak places them in a location in this diagram consistent with the rest of the rotation distribution.

There are some remaining outliers of note called out in Figure 6, which we now briefly discuss.

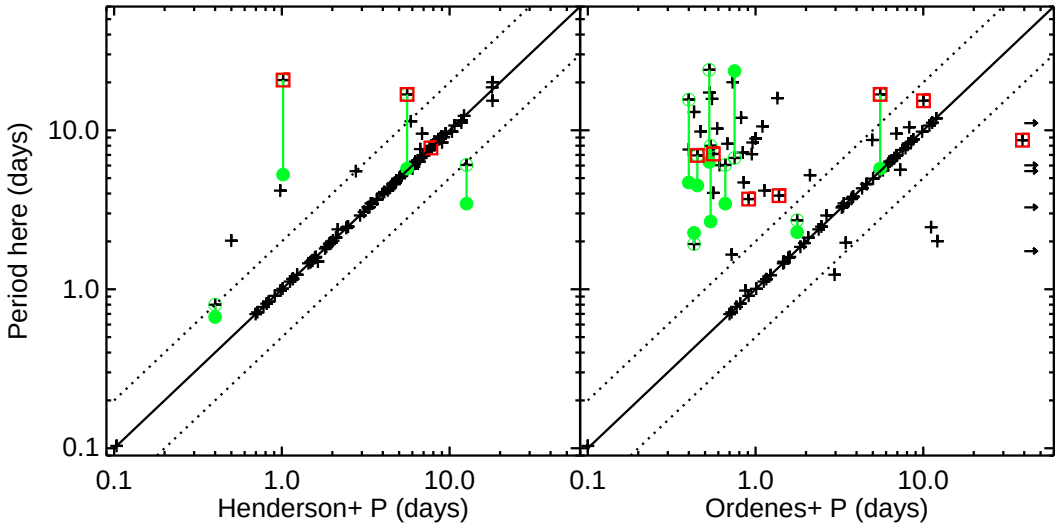

Figure 4. Comparison of periods obtained here (y-axis) to those in the literature (x-axis), C. B. Henderson & K. G. Stassun (2012) on the left and C. Ordenes-Huanca et al. (2022) on the right. The solid line is the 1:1 match, and dashed lines are a factor of 2 off. In general, the periods we report here are well-matched to those in the literature. Open green circles surround targets where the match to the first period we report is significantly different than the reported period, and they are linked with a solid green line to a filled-in circle at the location of the second period we report for that target, where available. In most cases, this second period moves the period reported here closer to those reported in the literature for that target. Additional red squares indicate periods that were tagged uncertain in our analysis (and are identified as such in our final catalog); they are occasionally good matches to the literature values. (There are 5 periods from C. Ordenes-Huanca et al. (2022) that are >100d, and would be off to the right here, represented by the right-pointing arrows.)

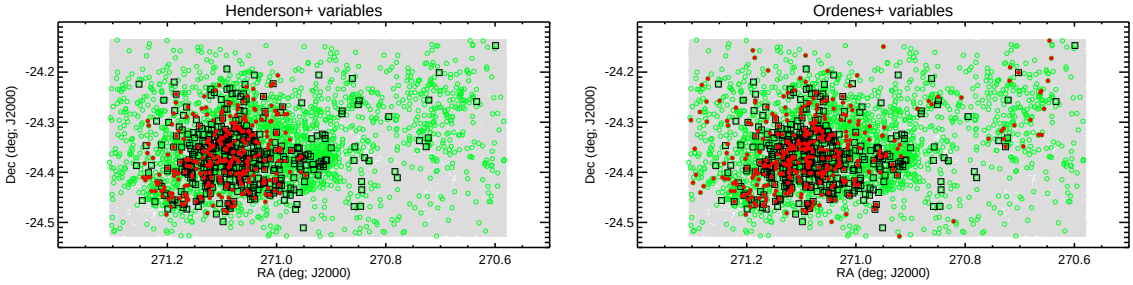

Figure 5. Location on the sky of stars from C. B. Henderson & K. G. Stassun (2012) on the left and C. Ordenes-Huanca et al. (2022) on the right, in red dots plotted on top of the whole catalog in small grey dots from L. M. Rebull et al. (2026), with open green circles around the YSOs from L. M. Rebull et al. (2026). Additional black squares are the stars with K2 light curves presented in this paper. C. B. Henderson & K. G. Stassun (2012) covers a smaller area than C. Ordenes-Huanca et al. (2022).

The star marked 1 is J180421.68-241547.0, and it has two periods, one very fast (as shown), and one ∼4.3 d. If we were to move this star to near 4 days in this plot, it would not be an outlier. The very fast peak is stronger in the periodogram than the 4 day peak, suggesting we should keep the faster period as the primary period. There is the very real question of whether or not this period should be identified with this star, or if source confusion is important here. The ZTF light curve for this source is not publicly accessible, but the ASAS-SN (B. J. Shappee et al. 2014; C. T. Christy et al. 2023) light curve is available, and also returns the fast period. Moreover, the ASAS-SN light curve's power spectrum does not have a peak consistent with the slower period at all. Thus, we have retained this star and this period here, but concede that it may be pulsation and not rotation.

The star marked 2 is J180325.93-242806.0 is a likely contact binary. We know from the Pleiades (J. Stauffer et al. 2016) that binaries are often fast-rotating outliers.

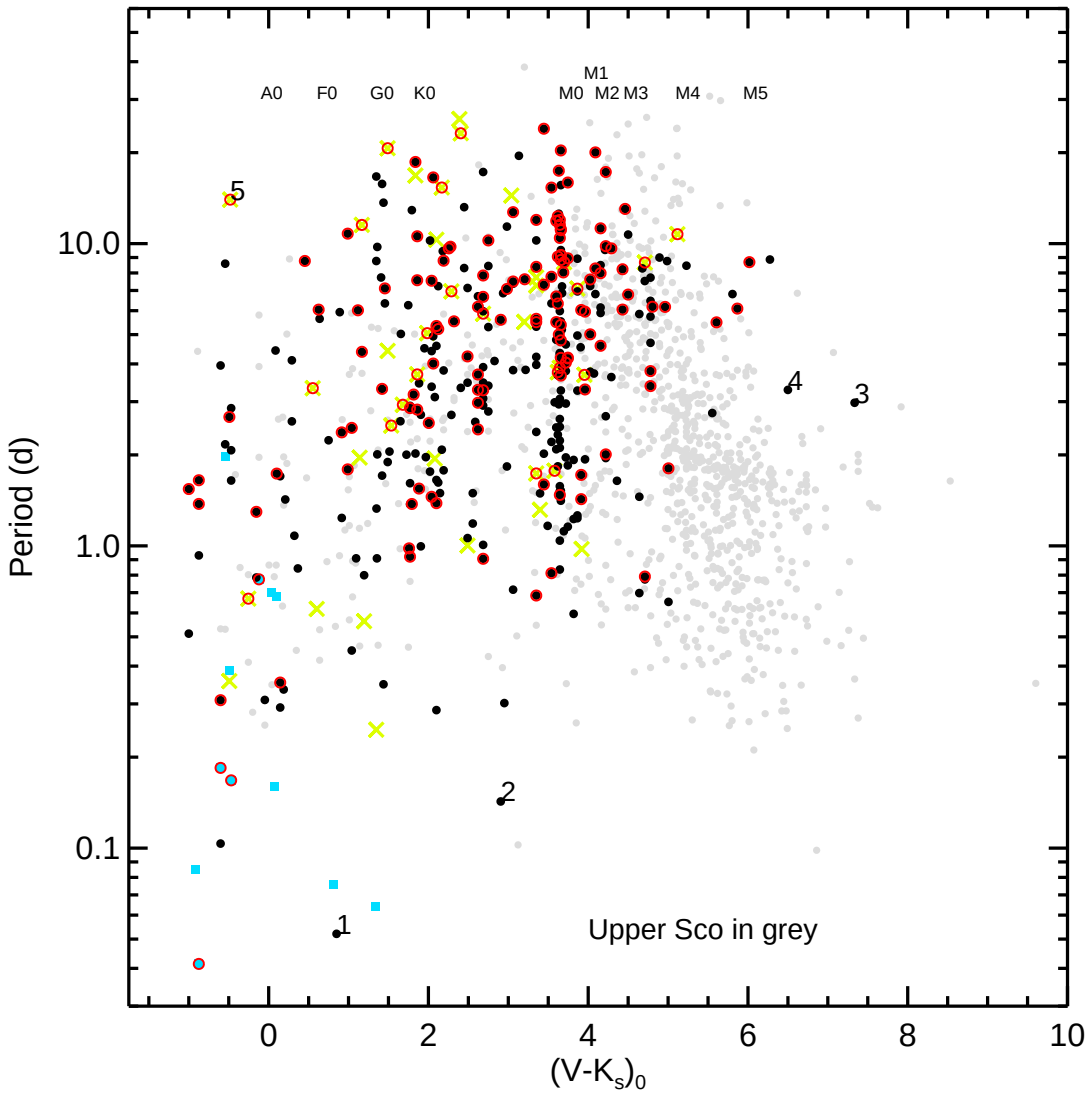

Figure 6. The distribution of rotation rates (in days) as a function of $(V - K_s)_0$ color as a proxy for mass in the Lagoon Nebula. Approximate spectral types as a function of color are given along the top of the plot. Cyan squares indicate stars whose periods we suspect may be pulsation (perhaps not rotation). Chartreuse × denote stars whose period may be less reliable than other stars here. An additional red circle around a point denotes an IR excess (a likely circumstellar disk). Grey points in the background come from Upper Scorpius (L. M. Rebull et al. 2018), and are there to guide the eye. Outliers are numbered; see the text. The overall structure of the distribution roughly matches that from USco – mid-K has the slowest rotators and both higher and lower masses rotate more quickly. See the text for more details.

There are two stars that are very red. The star marked 3 is J180358.81-242555.8 and while its rotation doesn't necessarily make it an outlier, its color does. The SED is well-behaved (implying that the V estimate is good), and there are two K_s measurements, from 2MASS and UKIDSS, very close to each other. Its placement in the JHK_s diagram suggests that there is IR excess that could be affecting K_s, which may explain its placement in $(V - K_s)_0$. The star marked 4 is J180405.41-242232.7, and again, its rotation doesn't particularly make it an outlier, but its color suggests extreme redness. There is some scatter in the SED, but the V estimate is probably accurate; the placement in JHK_s suggests that the K_s is photospheric. C. B. Henderson & K. G. Stassun (2012) reports the same period that we do for this star, suggesting the period is ok. We have no clear explanation for the location of this star.

The star marked 5 is J180450.61-242541.8 and the period we have for it, ∼14 d, suggests it is very slowly rotating given its color. This star has an unambiguous IR excess (disk) and its light curve suggests dust occultations. There are variations on multiple timescales. The longer period that we have tied to this star seems repeatable/reliable, but perhaps it is not stellar rotation. There is a period near ∼0.4 d that one can kind of identify by eye, but it is not reliable over the entire K2 campaign. Knowing that, one can look for a similar peak in the ZTF light curve, and it phases well, but one would not have selected that peak from ZTF without that prior knowledge. We have left this star at the ∼14 d period as a result, but it is possible that it should be tagged with a faster period.

3.2. *In Context with Other Young Clusters*

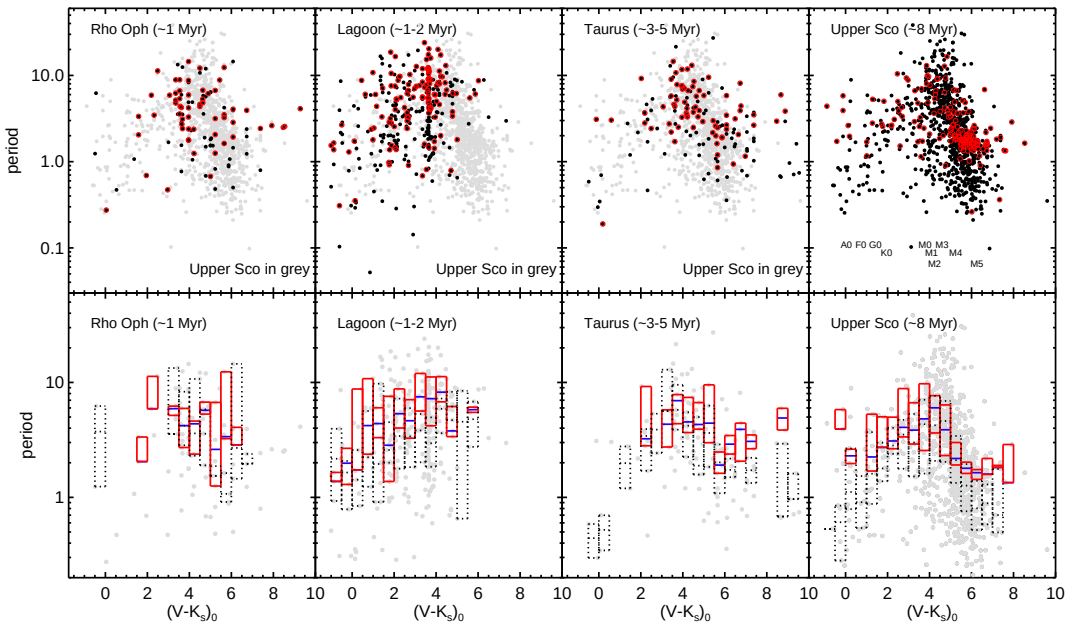

Figure 7. The distribution of rotation rates (in days) as a function of $(V - K_s)_0$ color as a proxy for mass in four clusters: ρ Oph (∼1 Myr), Lagoon (∼1-2 Myr), Taurus (∼3-5 Myr), and USco (∼8 Myr), as indicated; all of these are based on K2 data. In the top row, an additional red circle denotes an IR excess (at any band), *e.g.*, a disk. In the first three panels of the top row, the data from USco are plotted in grey to guide the eye. Pulsators and low-confidence members and periods are omitted from all panels. Approximate spectral types are indicated in the last panel of the top row. The bottom row is the same four clusters in the same order (note the y-axis is slightly reduced compared to the top row for clarity), but now the grey points are the corresponding cluster's points, and the boxes show the median, first, and 3rd quartile of the distribution within that color range. The red solid lines are disked stars (with the medians blue) and the black dotted lines are the disk-free stars. The new Lagoon data presented here represents a substantial addition to the known rotation rates for 1-5 Myr stars. The overall structure of the P vs. color distribution is similar across the four clusters. Disked rotation rates are slightly slower than that for disk-free. See the text for more details.

Figure 7 puts these Lagoon results in context with three other of our youngest clusters with K2 data, analyzed in exactly the same way: ρ Oph (∼1 Myr; L. M. Rebull et al. 2018), Taurus (∼3-5 Myr; L. M. Rebull et al. 2020), and USco (∼8 Myr; L. M. Rebull et al. 2018). The top row of Figure 7 has the clearest, best possible distributions and the bottom row has the medians, 25th, and 75th percentile of the distributions shown in $(V - K_s)_0$ color bins.

The first thing to notice is the number of points in each panel in the first row. The panel for USco is very well-populated – there are nearly 1000 stars in that plot, to be compared with ∼200 in Taurus, and ∼100 in ρ Oph. The 325 (high confidence, unlikely pulsator) stars that we can now add from the Lagoon represent a substantial addition to the distribution of K2 stellar rotation rates available for the ∼1-5 Myr population.

Unavoidably, ρ Oph, Taurus, and USco are only about ∼140 pc away, whereas the Lagoon is much further (∼1250 pc). Therefore, we are unable to probe very deeply into the lowest mass stars in the Lagoon, certainly in comparison

to these other three clusters. Figure 8 shows histograms of $(V - K_s)_0$ for the four clusters in Fig. 7. It is clear that the Lagoon data cut off in the early Ms whereas the rest of the clusters reach mid-Ms.

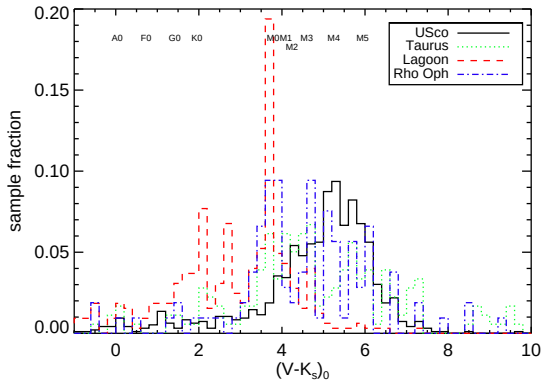

Figure 8. The distribution of $(V - K_s)_0$ colors for the stars with periods (those that appear in Fig. 7) in four clusters: ρ Oph (∼1 Myr; blue dash-dot), Lagoon (∼1-2 Myr; red dashed), Taurus (∼3-5 Myr; green dotted), and USco (∼8 Myr; black solid), as indicated. Approximate spectral types are shown across the top of the plot. It is again clear that data from the Lagoon do not reach as far into the M stars as the other clusters.

Another feature apparent in the rotation rate distribution is that despite selection effects imposed by fewer stars and the lower mass cutoff in the Lagoon, there is an overall similar structure in all four of these clusters – the slowest rotators are found near $(V - K_s)_0$∼3.5-4, with faster rotators both bluer and redder than that. Because there are many more stars in USco, that distribution is the most structured of the four, but based on the medians in the bottom row of Fig. 7, Taurus has that structure clearly in place as well. It is less evident in ρ Oph because there are fewer stars. The structure is even less obvious in the Lagoon, as a result of the many fewer mid- to late-M stars.

For all of these clusters, the light curves are space-based, so the periods are either known very precisely, typically to 0.001 d, or are incorrect by a significant margin (factor of 2 aliasing, simply wrong due to source confusion, or simply wrong due to stochastic noise most often from accretion/dust occultation in the light curves). Additionally, for all four of these clusters, reddening plays an important role. We have endeavored to mitigate this (see reddening discussions in the corresponding papers for the other clusters). The quantization in $(V - K_s)_0$ that comes from dereddening according to spectral types can be seen in at least three of the four clusters. However, there is an unavoidable effective smearing in the x-direction that must still be present in these plots, particularly in the first three relatively sparse and youngest (dustiest) clusters. It is encouraging that the overall structure nonetheless seems to still emerge in all of these clusters. It is, however, clearly noisy, particularly in the two youngest clusters, likely exacerbated by the relatively small sample size, variable reddening, and limited depth in the Lagoon.

3.3. *Influence of Disks*

Figure 7 also distinguishes between the disked and disk-free stars. For the Lagoon, there are a total of 124 disked stars and 201 disk-free stars with reliable rotation rates.

USco has so many M stars that no sophisticated statistics are required to detect the pile-up of disked M stars at ∼2d (also see discussion in L. M. Rebull et al. (2018)). It is obvious in the corresponding bins of the USco median plot that the ensemble of disked M stars tends on average to rotate more slowly than the disk-free M stars. This trend continues in the other clusters as well, but the sample sizes are much smaller, and so the significance is correspondingly weaker. The 75th percentile ends of the boxes for the disked stars always extend above that for the disk-free stars in USco $(V - K_s)_0$∼1-4. In Taurus, among the 10 bins where there are both disked and disk-free stars, seven have the 75th percentile end of the boxes for the disked stars extend above that for the disk-free. For the Lagoon, there are 13 bins where there are both disked and disk-free stars, and 9 have the 75th percentile end of the boxes for the disked stars extend above that for the disk-free stars. Among the Lagoon bins, the two bins that have the largest discrepancy between disked and disk-free are also the best-populated bins (*e.g.*, should be the most reliable).

We conclude that there is weak evidence that the disk-bearing stars rotate, on average, more slowly than the disk-free stars, particularly in the late K/early M regime, even for stars as young as in the Lagoon. Assessing this in any

more detail is greatly complicated by the relatively small sample sizes found in the youngest three clusters, and the uncertainties of dereddening, as well as the fact that stars with disks often have complex light curves where periods are harder to extract; see next section.

4. OTHER LIGHT CURVE PROPERTIES

4.1. *Dippers and Bursters and Other Disk-Influenced Light Curves*

L. Venuti et al. (2021) discussed the multi-color variability properties of the light curves, particularly of the disked population, so we make only limited comments here.

Of the 16 stars we have identified as likely bursters, all but one of them are also (independently) identified as having an IR excess (circumstellar disk). However, that one apparent disk-free star (J180407.27-242527.6) has very few points longer than 2 μm, and in the context of the rest of the full ensemble of stars considered in L. M. Rebull et al. (2026), any evidence for (or against) an IR excess is very weak.

Of the 39 stars we have identified as likely dippers, similarly most of them are also (independently) identified as having an IR excess (circumstellar disk). Of the 6 that are not tagged as having a disk, 1 has no data past 2 μm, 2 are subject to the systematic IRAC offset (see above), and the remaining 3 similarly have simply weak (or ambiguous) evidence for an IR excess.

We have tagged 91 stars as generally having light curve patterns consistent with other stars that have disks; all but 11 independently have IR excesses.

Figure 9 shows that these objects with light curves suggestive of disks have a vague tendency towards longer periods, consistent with above when we considered solely those with IR excesses.

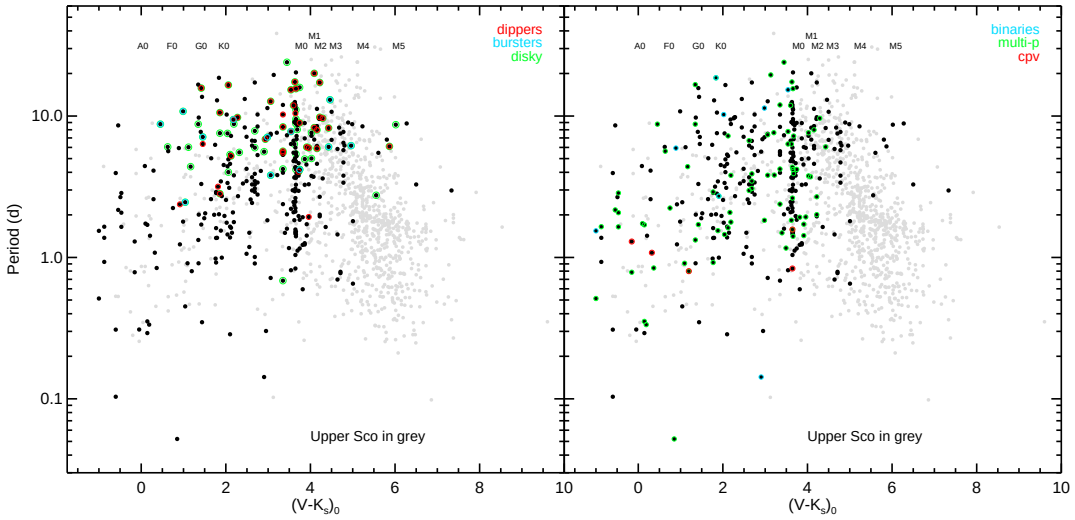

Figure 9. Another view of P vs. $(V - K_s)_0$ color, as before (with uncertain ('iffy') and pulsating periods removed), but with dippers (red), bursters (blue), and with characteristics similar to that of stars having disks ('disky'; green) light curves highlighted on the left, and binaries (blue), multi-periodic stars (green), and CPVs (red; see Sec. 4.3) highlighted on the right. Stars with indications of having a disk (light curves suggesting presence of a disk, e.g., really anything in the left panel) tend towards longer periods. Binaries in other clusters tend to be the fast outliers, but apparently not always here; just one is a fast outlier. CPVs are biased towards fast periods but are not M stars per se. Multi-periodic stars are found throughout the brighter stars; presumably the fainter stars have light curves that are too noisy to easily reveal multiple periods. See the text for more details.

4.2. *Multi-Periodic Stars & Binaries*

Photometric binary stars in the Pleiades tend to be fast-rotating outliers (J. Stauffer et al. 2016). It is, however, far easier to identify photometric binaries in the Pleiades than it is in the Lagoon or other very young clusters where the stars are not only subject to reddening but also have not yet settled into a narrow isochrone at the main sequence. We

can identify nine eclipsing binaries, or possible eclipsing binary candidates, in our Lagoon sample. In several cases, the period we report here is obtained by omitting the eclipses and searching for periods in what, presumably, is the remaining photospheric signal. (These cases are noted in the table.) These binaries do not particularly seem to be rotating quickly, except for the one outlier noted in Sec. 3.1 above.

In USco (L. M. Rebull et al. 2018), UCL/LCC (L. M. Rebull et al. 2022), the Pleiades (L. M. Rebull et al. 2016), and Praesepe (L. M. Rebull et al. 2017), multi-periodic M stars were often likely binary M stars; higher-mass multi-periodic stars could suggest binarity or could be multiple spot/spot groups differentially rotating on a single star. Here in the Lagoon, as seen in Figure 9, there are few multi-periodic stars with $(V - K_s)_0 \gtrsim 4.5$, presumably mostly due to the fact that the stars are too faint for multiple periods to be easily extracted from the light curve. Bluer than that, however, there are multi-periodic stars scattered through the distribution. In upcoming work, we analyze speckle photometry to further tease out the effect of multiplicity on periodic and other variability types.

4.3. *CPVs*

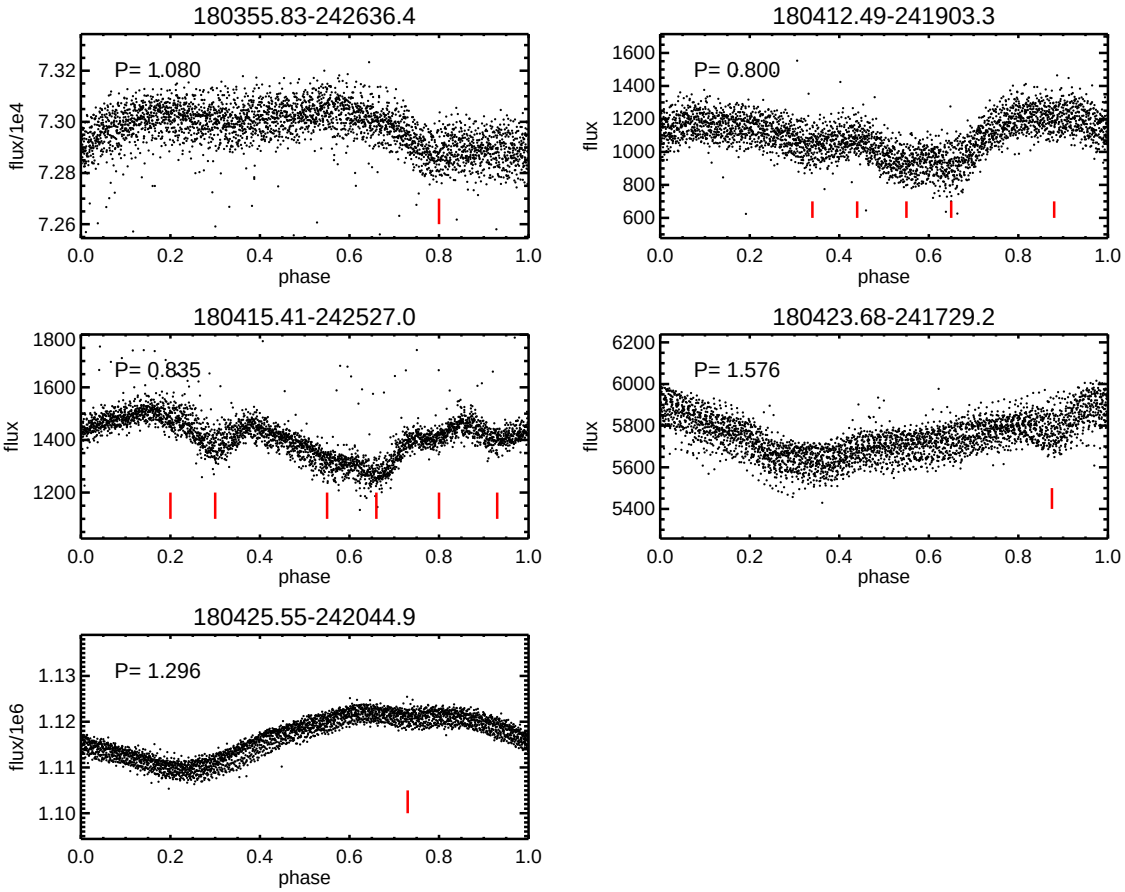

Figure 10. Phased light curves for the CPVs discussed in Sec. 4.3, in the same order as they appear in the text. Red hash marks indicate the location of the sharp-edged dips. The last one is the earliest spectral type (a B star) and is least like a CPV in shape. See the text for more details.

Based on K2 data, we identified a class of light curves that we suspect are a result of orbiting clouds of material (J. Stauffer et al. 2017, 2018, 2021). In J. Stauffer et al. (2017), the objects were defined as being all young, disk-free, rapidly rotating M stars, and placed into categories dubbed 'scallop shells', 'persistent flux-dip', or 'transient narrow dip.' Scallop shells were required to have periods less than 0.65 days.

As the hunt for these kinds of objects expanded (e.g., L. G. Bouma et al. 2024; L. G. Bouma & M. M. Jardine 2025; S. Daley-Yates et al. 2026), the nomenclature changed to "complex periodic variables (CPVs)" because the light curve shapes – with sharp-edged structure – resulted in power spectra with many peaks, most of which are harmonics of

the main period. The definition expanded slightly to no longer require that the stars have P <0.65 d or strictly be M stars, though the basic physical interpretation of orbiting clouds of material has persisted.

There are five stars in the Lagoon that bear hallmarks of these kinds of light curves, though some are confusing, and none are M stars. Since all of these stars are earlier types (three far earlier type) than the 'classical' requirement of an M star, perhaps they are not CPVs at all. Or, it's possible that these stars are multiples of some sort and the companion is the CPV. If this is the case, the high mass star would contribute little or no variability to the light curve, and the CPV portion of the light curve would come from the later-type companion. For the four of these that have Gaia data, Gaia does not indicate (via RUWE) that they are multiples (though these stars may well be too far away for RUWE to be helpful). Moreover, the amplitude of the variability suggests that companions can't be responsible.

We now discuss each of these stars. They are plotted in the P vs. $(V-K_s)_0$ diagram in Fig. 9, where they clearly skew towards faster rotation in general, but not all as fast as 0.65 d. The phased light curves appear in Fig. 10, in the same order in which they appear here, with the angular dips indicated.

J180355.83-242636.4: This star is a A3.75 (L. Venuti et al. 2024), so the $(V-K_s)_0$ is 0.322. It has been identified by five different studies as a YSO, largely but not exclusively on the basis of X-rays. It does not have compelling evidence for a circumstellar disk – IRAC-3 is significantly above the photosphere, and there is a MIPS-24 limit near the photosphere, suggesting that the IRAC-3 point is erroneous. The light curve has many low drops below the continuum (cropped out of Fig. 10), as if they were short eclipses, but we could find no period that would synch them. There is clear angular structure in the main portion of the light curve resulting in many harmonic peaks in the power spectrum, resulting in this star being classified as a CPV. However, its main rotation period is 1.080 d, longer than the 'classical' definition. This star is bright, and in a region of sky with high surface brightness, such that we do not have a lot of optical data for it (including no Gaia data), so it is difficult to constrain based on ancillary data whether or not it has a companion.

J180412.49-241903.3: L. Venuti et al. (2024) has this star as F5.5, meaning that its $(V-K_s)_0$ is 1.195. This star is unlikely to have an IR excess, but the IR is systematically offset from a Rayleigh-Jeans line extended from K_s (see discussion in L. M. Rebull et al. (2026)). It is identified by seven different papers in the literature as a YSO. This light curve is a stereotypical CPV shape, albeit noisy, with several angular dips per cycle; at 0.800 d, it is a little slow compared to the 'classical' definition, but as an F star, it is also more massive.

J180415.41-242527.0: This star has been identified by 10 different articles as a YSO. L. Venuti et al. (2024) classifies it as a K7.5, so its $(V-K_s)_0$ is 3.645. It does not appear to have an IR excess. This star also has a stereotypical CPV light curve shape, with several sharp, angular dips per cycle. It, too, is a bit slow at 0.835 d. It has a few obvious flares during the observing campaign. This is one of the latest-type CPV stars we have identified, and thus closest to the 'classical' definition.

J180423.68-241729.2: This is also a K7.5 (L. Venuti et al. 2024) and therefore has $(V-K_s)_0$= 3.645; it is identified by 12 different papers as a likely YSO. It does not appear to have an IR excess. At 1.576 d, its period is fairly long for a CPV. Its light curve is more ambiguous than the other CPV candidates here, less obviously CPV. It has one dip that is angular enough to produce several harmonic peaks in the periodogram.

J180425.55-242044.9: This is the most confusing of the stars in this list. L. Venuti et al. (2024) has it as a B8.75, and it appears to have a circumstellar disk, with a significant IR excess at least at 8 and 24 μm if not 5.8 μm as well. It's been identified by 7 studies as a YSO. It has a period of 1.296 d, so very slow for a CPV. It does not have myriad peaks in the periodogram, but it does have a somewhat angular dip in the phased light curve, which is why we initially tentatively put it in this class (initial classifications of light curves are done independently of any other information about the object such as spectral type). Since it is a B star, has a disk, and the period is so long, plus the fact that its light curve shape is the least stereotypically CPV of all of them here, all of this suggests that perhaps it should not be in the CPV class – maybe the structure is an eclipse and/or it is a binary instead. However, it could also be of the family of high-mass analogs mentioned in L. G. Bouma & M. M. Jardine (2025).

From our work in other clusters, we expect a higher rate of these kinds of CPVs in younger clusters – ∼1% of Pleiades stars, ∼3% of UCL/LCC, ∼3% of USco, and ∼4% of Taurus stars are like this. Out of the best sample of stars with good rotation periods and colors, there are 325 Lagoon stars, and if 4 or 5 of them are CPVs, that's just ∼1-2%. However, the prior definition required that CPV stars be M stars, and all of the prior cluster data had many more M stars, so it is less surprising that the sample fraction for the Lagoon is different.

5. SUMMARY

In this paper, we have worked with 414 K2 light curves for young stars in the Lagoon Nebula, one of the youngest (∼1-2 Myr; L. Prisinzano et al. 2019) clusters with space-based rotation rates available. We find 376 periods, 325 of which are unambigous periods and likely rotation (as opposed to pulsation). Since the cluster is at ∼1250 pc (L. Prisinzano et al. 2019), the faintest available rotation rates only reach the earliest M stars. The overall structure is broadly consistent with expectations in that the slowest rotation rates are near mid-K, with both higher and lower masses rotating faster. Out of the 325 highest quality rotation periods, 124 are disk-bearing and 201 are disk-free. There is some weak evidence that stars with disks may be rotating slower on average, but there are simply not enough stars to assert this with any confidence. Multiperiodic stars are located throughout the distribution.

There are a handful of CPV stars, which is not surprising because the Lagoon is young, but what is surprising is that none of these CPV stars are M stars – they are all mid-K or earlier. It's possible that the stars creating the CPV structure in the light curves are unseen low-mass companions, or the stars we have identified here as CPVs are not true CPVs, but something other than the M stars that have been previously used to define the CPV category.

ACKNOWLEDGMENTS

- This research has made use of the NASA/ IPAC Infrared Science Archive (IRSA), which is operated by the Jet Propulsion Laboratory, California Institute of Technology, under contract with the National Aeronautics and Space Administration.
- This paper includes data collected by the Kepler mission and obtained from the MAST data archive at the Space Telescope Science Institute (STScI). Funding for the Kepler mission is provided by the NASA Science Mission Directorate. STScI is operated by the Association of Universities for Research in Astronomy, Inc., under NASA contract NAS 5–26555.
- ZTF is supported by the National Science Foundation and a collaboration including current partners Caltech, IPAC, the Oskar Klein Center at Stockholm University, the University of Maryland, the University of California at Berkeley, the University of Wisconsin at Milwaukee, University of Warwick, Ruhr University, Cornell University, Northwestern University and Drexel University. Operations are conducted by COO, IPAC, and UW.
- This publication makes use of data products from the Wide-field Infrared Survey Explorer (WISE), which is a joint project of the University of California, Los Angeles, and the Jet Propulsion Laboratory/California Institute of Technology, funded by the National Aeronautics and Space Administration.
- This work is based in part on archival data obtained with the Spitzer Space Telescope, which was operated by the Jet Propulsion Laboratory, California Institute of Technology under a contract with NASA.
- This publication makes use of data products from the Two Micron All Sky Survey (2MASS), which is a joint project of the University of Massachusetts and the Infrared Processing and Analysis Center/California Institute of Technology, funded by the National Aeronautics and Space Administration and the National Science Foundation.
- Herschel is an ESA space observatory with science instruments provided by European-led Principal Investigator consortia and with important participation from NASA.
- This research made use of data products from the Midcourse Space Experiment (MSX). Processing of the data was funded by the Ballistic Missile Defense Organization with additional support from NASA Office of Space Science.
- The Pan-STARRS1 Surveys (PS1) and the PS1 public science archive have been made possible through contributions by the Institute for Astronomy, the University of Hawaii, the Pan-STARRS Project Office, the Max-Planck Society and its participating institutes, the Max Planck Institute for Astronomy, Heidelberg and the Max Planck Institute for Extraterrestrial Physics, Garching, The Johns Hopkins University, Durham University, the University of Edinburgh, the Queen's University Belfast, the Harvard-Smithsonian Center for Astrophysics, the Las Cumbres Observatory Global Telescope Network Incorporated, the National Central University of Taiwan,

the Space Telescope Science Institute, the National Aeronautics and Space Administration under Grant No. NNX08AR22G issued through the Planetary Science Division of the NASA Science Mission Directorate, the National Science Foundation Grant No. AST–1238877, the University of Maryland, Eotvos Lorand University (ELTE), the Los Alamos National Laboratory, and the Gordon and Betty Moore Foundation.

- This work is based in part on data obtained as part of the UKIRT Infrared Deep Sky Survey (UKIDSS).
- This work has made use of data from the European Space Agency (ESA) mission *Gaia* (https://www.cosmos.esa.int/gaia), processed by the *Gaia* Data Processing and Analysis Consortium (DPAC, https://www.cosmos.esa.int/web/gaia/dpac/consortium). Funding for the DPAC has been provided by national institutions, in particular the institutions participating in the *Gaia* Multilateral Agreement.
- The VVV is based on data products from observations made with ESO Telescopes at the La Silla Paranal Observatory under programme ID 179.B-2002
- The VPHAS catalogue is based on data products from observations made with ESO Telescopes at the La Silla Paranal Observatory under public survey programme ID, 177.D-3023
- This work was partially supported by the National Aeronautics and Space Administration (NASA) under grant No. 80NSSC21K0633 issued through the NNH20ZDA001N Astrophysics Data Analysis Program (ADAP).
- Machine learning tools were used to suggest language improvements within the manuscript. Responsibility for the final manuscript text lies entirely with the authors.

Thanks for everything, Mom. Miss you.

AUTHOR CONTRIBUTIONS

Co-Author Cody reduced the light curves from K2. Co-Author A. Thanvantri worked on the PSF-fitted light curves, and Co-Author S. Thanvantri did an early analysis of the rotation periods. Co-Author Venuti analyzed the light curves initially in L. Venuti et al. (2021). Author Rebull analyzed and classified the K2 light curves in exactly the same way as other papers in her series of K2 rotation periods; she combined it with the catalog from L. M. Rebull et al. (2026), then did the remaining analysis and wrote the paper. Co-authors Cody and Venuti helped resolve discrepancies between the papers and commented on the manuscript.

Facility: IRSA

REFERENCES

2MASS Team. 2020, 2MASS Survey Merged Point Source Information Table,, NASA IPAC DataSet, IRSA110 doi: 10.26131/IRSA110

Akeson, R. L., Chen, X., Ciardi, D., et al. 2013, PASP, 125, 989, doi: 10.1086/672273

Bellm, E. C., Kulkarni, S. R., Graham, M. J., et al. 2019, PASP, 131, 018002, doi: 10.1088/1538-3873/aaecbe

Bouma, L. G., & Jardine, M. M. 2025, ApJL, 988, L3, doi: 10.3847/2041-8213/ade39a

Bouma, L. G., Jayaraman, R., Rappaport, S., et al. 2024, AJ, 167, 38, doi: 10.3847/1538-3881/ad0c4c

Cardelli, J. A., Clayton, G. C., & Mathis, J. S. 1989, ApJ, 345, 245, doi: 10.1086/167900

Christy, C. T., Jayasinghe, T., Stanek, K. Z., et al. 2023, MNRAS, 519, 5271, doi: 10.1093/mnras/stac3801

Cody, A. M., & Hillenbrand, L. A. 2018, AJ, 156, 71, doi: 10.3847/1538-3881/aacead

Cody, A. M., Hillenbrand, L. A., & Rebull, L. M. 2022, AJ, 163, 212, doi: 10.3847/1538-3881/ac5b73

Cody, A. M., Venuti, L., & Thanvantri, A. 2023, Data from Light curves of young stars from K2 (K2YSO),, https://archive.stsci.edu/hlsp/k2yso doi: 10.17909/44f5-5e13

Daley-Yates, S., Jardine, M. M., & Bouma, L. 2026, MNRAS, 549, stag837, doi: 10.1093/mnras/stag837

Henderson, C. B., & Stassun, K. G. 2012, ApJ, 747, 51, doi: 10.1088/0004-637X/747/1/51

Howell, S. B., Sobeck, C., Haas, M., et al. 2014, PASP, 126, 398, doi: 10.1086/676406

Indebetouw, R., Whitney, B. A., Kawamura, A., et al. 2008, AJ, 136, 1442, doi: 10.1088/0004-6256/136/4/1442

Kochanek, C. S., Shappee, B. J., Stanek, K. Z., et al. 2017, PASP, 129, 104502, doi: 10.1088/1538-3873/aa80d9

Masci, F. J., Laher, R. R., Rusholme, B., et al. 2019, PASP, 131, 018003, doi: 10.1088/1538-3873/aae8ac

Meyer, M. R., Calvet, N., & Hillenbrand, L. A. 1997, AJ, 114, 288, doi: 10.1086/118474

Minniti, D., Lucas, P., & Vvv Team. 2017, VizieR Online Data Catalog: VISTA Variable in the Via Lactea Survey DR2 (Minniti+, 2017),, VizieR On-line Data Catalog: II/348. Originally published in: Astron. Astrophys., 537, A107 (2002)

Ordenes-Huanca, C., Zoccali, M., Bayo, A., et al. 2022, MNRAS, 517, 6191, doi: 10.1093/mnras/stac3049

Pecaut, M. J., & Mamajek, E. E. 2013, ApJS, 208, 9, doi: 10.1088/0067-0049/208/1/9

Prisinzano, L., Damiani, F., Kalari, V., et al. 2019, A&A, 623, A159, doi: 10.1051/0004-6361/201834870

Rebull, L. M., Stauffer, J. R., Cody, A. M., et al. 2020, AJ, 159, 273, doi: 10.3847/1538-3881/ab893c

Rebull, L. M., Stauffer, J. R., Cody, A. M., et al. 2018, AJ, 155, 196, doi: 10.3847/1538-3881/aab605

Rebull, L. M., Stauffer, J. R., Hillenbrand, L. A., et al. 2017, ApJ, 839, 92, doi: 10.3847/1538-4357/aa6aa4

Rebull, L. M., Stauffer, J. R., Hillenbrand, L. A., et al. 2022, AJ, 164, 80, doi: 10.3847/1538-3881/ac75f1

Rebull, L. M., Venuti, L., & Cody, A. M. 2026, AJ, submitted

Rebull, L. M., Stauffer, J. R., Bouvier, J., et al. 2016, AJ, 152, 114, doi: 10.3847/0004-6256/152/5/114

Saito, R. K., Hempel, M., Minniti, D., et al. 2012, A&A, 537, A107, doi: 10.1051/0004-6361/201118407

Scargle, J. D. 1982, ApJ, 263, 835, doi: 10.1086/160554

Shappee, B. J., Prieto, J. L., Grupe, D., et al. 2014, ApJ, 788, 48, doi: 10.1088/0004-637X/788/1/48

Skrutskie, M. F., Cutri, R. M., Stiening, R., et al. 2006, AJ, 131, 1163, doi: 10.1086/498708

Stauffer, J., Rebull, L., Bouvier, J., et al. 2016, AJ, 152, 115, doi: 10.3847/0004-6256/152/5/115

Stauffer, J., Collier Cameron, A., Jardine, M., et al. 2017, AJ, 153, 152, doi: 10.3847/1538-3881/aa5eb9

Stauffer, J., Rebull, L., David, T. J., et al. 2018, AJ, 155, 63, doi: 10.3847/1538-3881/aaa19d

Stauffer, J., Rebull, L. M., Jardine, M., et al. 2021, AJ, 161, 60, doi: 10.3847/1538-3881/abc7c6

Venuti, L., Cody, A. M., Rebull, L. M., et al. 2021, AJ, 162, 101, doi: 10.3847/1538-3881/ac0536

Venuti, L., Cody, A. M., Beccari, G., et al. 2024, AJ, 167, 120, doi: 10.3847/1538-3881/ad1f65

ZTF Team. 2026, ZTF Lightcurves,, NASA IPAC DataSet, IRSA598 doi: 10.26131/IRSA598